Fabrication of ZnSe Microlens Array for a Wide Infrared Spectral Region

Fan Zhang, Qing Yang, Hao Bian, Feng Liu, Minjing Li, Xun Hou, and Feng Chen

***Abstract*— The infrared (IR) is a strategically important band for numerous applications from environment to biochemical imaging. Here a novel IR optical component integrates more than 2000 plano-concave microlenses on the zinc selenide (ZnSe) surface within a footprint of $5 \times 5\text{mm}^2$ is proposed by a combined method of femtosecond laser direct irradiation and chemical wet etching. Microlenses with diameter from 15 to 30 μm are realized by controlling the laser power and etching time. The uniform close-packed microlens arrays (MLAs) with minimized volume and high transparency at wavelengths of 0.76∼22μm are realized. The MLAs have relatively good topography and surface quality. The modulation transfer function (MTF), imaging test and optical-focusing test confirm the outstanding IR imaging. Owing to the merits of micro-size, light weight, high integration and excellent IR imaging performance, the as-fabricated MLA is promising in cutting-edge mid-IR and far-IR application, such as IR sensing system, imaging system, and so on.**

***Index Terms*— Infrared optics, femtosecond laser machining, wet etching, microlens array, ZnSe.**

Manuscript received May 24, 2020; revised July 3, 2020; accepted August 24, 2020. Date of publication September 4, 2020; date of current version September 25, 2020. This work was supported in part by the National Natural Science Foundation of China under Grant 61875158, Grant U1630111, Grant 51975460, and Grant 61435005; in part by the National Key Research and Development Program of China under Grant 2017YFB1104700; in part by the Open Project Program of the Wuhan National Laboratory for Optoelectronics under Grant 2018WNLOKF003; in part by the Shaanxi Province Science Foundation under Grant 2020JM-071; and in part by the Fundamental Research Funds for the Central Universities, Instrument Analysis Center of Xi'an Jiaotong University. *(Corresponding authors: Feng Chen; Hao Bian.)*

Fan Zhang, Feng Liu, and Feng Chen are with the State Key Laboratory for Manufacturing System Engineering, Xi'an Jiaotong University, Xi'an 710049, China, also with the Shaanxi Key Laboratory of Photonics Technology for Information, Faculty of Electronic and Information Engineering, School of Electronic Science and Engineering, Xi'an Jiaotong University, Xi'an 710049, China, and also with the International Joint Research Laboratory for Micro/Nano Manufacturing and Measurement Technologies, Xi'an Jiaotong University, Xi'an 710049, China (e-mail: chenfeng@mail.xjtu.edu.cn).

Qing Yang and Minjing Li are with the State Key Laboratory for Manufacturing System Engineering, Xi'an Jiaotong University, Xi'an 710049, China, also with the Shaanxi Key Laboratory of Photonics Technology for Information, Faculty of Electronic and Information Engineering, School of Electronic Science and Engineering, Xi'an Jiaotong University, Xi'an 710049, China, and also with the School of Mechanical Engineering, Xi'an Jiaotong University, Xi'an 710049, China.

Hao Bian is with the State Key Laboratory for Manufacturing System Engineering, Xi'an Jiaotong University, Xi'an 710049, China, also with the Shaanxi Key Laboratory of Photonics Technology for Information, Faculty of Electronic and Information Engineering, School of Electronic Science and Engineering, Xi'an Jiaotong University, Xi'an 710049, China, also with the International Joint Research Laboratory for Micro/Nano Manufacturing and Measurement Technologies, Xi'an Jiaotong University, Xi'an 710049, China, and also with the Wuhan National Laboratory for Optoelectronics, Huazhong University of Science and Technology, Wuhan 430074, China (e-mail: haobian@mail.xjtu.edu.cn).

Xun Hou is with the International Joint Research Laboratory for Micro/Nano Manufacturing and Measurement Technologies, Xi'an Jiaotong University, Xi'an 710049, China.

Color versions of one or more of the figures in this letter are available online at http://ieeexplore.ieee.org.

Digital Object Identifier 10.1109/LPT.2020.3021131

I. Introduction

MLAs operating in the mid-IR and far-IR have recently attracted increasing attention for their important applications in optical system, micro-manufacturing and biochemical systems [1], [2]. However, both the material and the manufacturing methods made the IR lens extremely complicated and time-consuming. For example, the mostly used IR materials are silicon and germanium. The lens are usually made by complex techniques with poor inefficiency, such as ultraprecision mechanical cutting [3] and mask-assisted etching [4]. And the concave or negative MLAs are not availably fabricated by those well-established techniques, which have extensive applications such as beam shaping [5], fluorescence biosensors [6]–[8] and carriers of DNA chips [9]. And they can integrate with other optical elements, can be applied in optical devices such as diffusers and scanners [10]. The situation becomes worse when further miniaturization or integration of other optical components is needed. Therefore, the limiting factor in the development of mid-IR and long-IR microlens array is the suitable fabrication methods for materials that are transparent in mid-wave and long-wave, low cost, and easy to machine [11].

ZnSe has many important optical properties, such as broad transparency from visible to mid-IR wavelengths and far-IR wavelengths, high refractive index, low dispersion and environment adaptiveness makes it an ideal IR optoelectronic material [12], [13]. However, from the perspective of micromachining, ZnSe is difficult to process using traditional technologies due to its brittleness. Generally, the common method is single point diamond turning (SPDT) which is only suitable for lens with normal size and time-consuming. Additionally, complex and high-cost procedures also limit its practical applications. As an appealing alternative, femtosecond laser fabrication has emerged as a powerful tool based on a wide range of materials, including metal, semiconductor and dielectric [14]. Previous works reported by our group and others have already proven the strong capability of the femtosecond laser in fabricating optical microdevices. For example, Wu *et al.* used femtosecond-laser-induced two-photon polymerization (TPP) method to fabricate hexagonal MLAs with 100% fill factor [15]. Sun *et al.* reported a femtosecond laser modification with subsequent ion beam etching technology for the fabrication of nanosmooth concave microlens arrays on hard materials [16]. Especially, the combination of femtosecond laser ablation and etching technologies enables mask-free fabrication of arbitrarily shaped optical devices with a reasonably smooth surface. At present, etching-assisted femtosecond laser machining has been considered a preferred strategy for fabricating high-quality optical components.

Herein, we report the design and experimental demonstration of high-efficiency IR microlens on the ZnSe surface

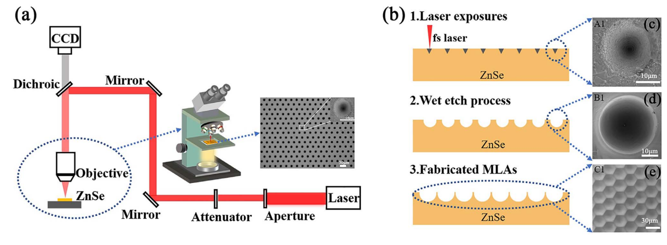

Fig. 1. Experiment configuration of the fabrication process. (a) Schematic of the system. Inset, array of pulse-irradiated craters. (b) Schematic illustration of the fabrication procedure. (c) SEM image of laser-induced micro-crater. (d) SEM image of concave microstructure. (e) SEM image of the formed IR MLA.

(II-VI Incorporated , USA) by femtosecond laser assisted chemical etching. The femtosecond laser pulse irradiation was focused on the surface of ZnSe glass, which contributed to induced stress [17], structural changes, and amorphization in the ZnSe glass, resulting in local chemical activity enhancement. Microlens arrays could be fabricated from crater arrays after chemical etching with a mixture of potassium permanganate powder ($KMnO_4$ 60mg) and concentrated sulfuric acid (H_2SO_4 5%) at room temperature. The morphology could be controlled by changing the laser power and etching time, the diameter of the microlens varied from 15μm to 30μm, the array with fill factors of up to 100%. The thousands concave microlens array fabricated efficiently using the method performed well in imaging and focusing tasks. The results indicate that the combination of femtosecond laser and chemical etching technology may open new possibilities for the fabrication of ZnSe-based optical devices.

II. Experiments

Fig. 1(a) shows the schematic diagram of femtosecond laser micro-machining set up. The commercial ZnSe glass substrate (II-VI Incorporated, USA) with dimensions of $5 \times 5 \times 1$ mm^3 was used in the experiment. After ultrasonic cleaning in deionized water for 10 minutes and dried in ambient air, the sample was mounted onto a three-axis stage. The femtosecond laser pulses, generated by an amplified Ti: sapphire laser system (Coherent Libra-usp-he, central wavelength of 800nm, pulse duration of 50 fs, repetition rate of 1 kHz), were focused onto the surface of ZnSe by an objective lens (Nikon, 5×, NA=0.15). The laser exposure process was monitored by a CCD sensor (Nikon DS-Vi1). The laser power and irradiation time were controlled by a variable density filter and a fast mechanical shutter.

The fabrication process for the concave microstructure is shown in Fig. 1(b). The first step was the focused laser irradiation on the surface of the ZnSe substrates to induce local material modification. The energy of the incident laser pulse, which could be controlled by the variable neutral density filter, was set to 3mW. A breakdown-induced crater could be created by 0.2 s exposure, which was controlled by a mechanical shutter. After the laser irradiation, it was critical to find an efficient route for the selective and efficient removal of the irradiation area. Previously attempted to remove this area by using acidic etching or highly toxic organic compounds had been reported but so far with moderate impact [18]. A new oxidizing route to ensure efficient removal of irradiation crater was presented based on the treatment with a mixture of an oxidizing agent for ZnSe [19]. This approach relies on the use of conventional, inexpensive, and relatively low toxic oxidizing agents, $KMnO_4$ in H_2SO_4. Herein, the etchant was optimized as 5% H_2SO_4 of 100ml and 60mg $KMnO_4$. In the initial phase of the etching, the laser-modified region [Fig. 1(c)] had a much higher selective etching rate than the un-irradiated regions, the concave microstructures [Fig. 1(d)] would be created in the laser-irradiated zone and evenly expanded until the laser-modified materials had been totally etched out. Sequentially, the aperture diameter of the circular microlenses expanded gradually with the ongoing chemical etching, and eventually the adjacent zones "overlapped" with each other, the surface profile of the IR MLA was observed by the scanning electron microscope (SEM, FEOLJSM-7000F), as shown in Fig. 1(e), the fill factor approached 100%.

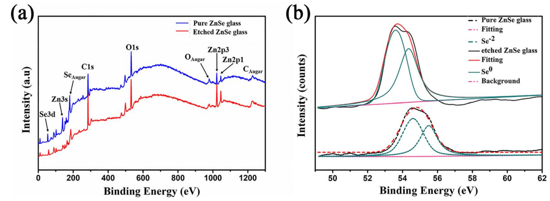

Fig. 2. High-resolution XPS spectra. (a) The full spectrum diagram of pure ZnSe glass and etched ZnSe glass. (b) The spectra for Se 3d region as pure ZnSe glass and etched ZnSe glass.

III. Results and Discussion

To identify the changes undergone by the main element involved in the proposed chemical processes, it is important to analyze the types of the elements and the change of the valence state of the element. Fig. 2(a) shows the full spectrum diagram, the elements of the etched ZnSe glass are the same as those of the pure ZnSe glass. The peaks of C and O elements in the samples indicate the H_2O, CO_2 and O_2 from ambient environment. In Fig. 2(b), X-ray photoelectron spectroscopy (XPS) spectra of the Se 3d region are presented for raw spectrum and etched with $KMnO_4/H_2SO_4$. Clear differences are observed in the Se signal from Fig. 2(a) and 2(b). After etching with $KMnO_4/H_2SO_4$, the doublet attributed to the valence 2- state is significantly reduced, whereas a doublet assigned to Se^0 dominates the XPS spectrum. This confirms that $KMnO_4/H_2SO_4$ induces oxidation of Se^{-2} to Se^0. The XPS Zn^{2+} signal decreases in this sample, thus confirming that changes in the valence state of Se are related to the transformation of ZnSe into elemental Se and Zn soluble species. Based on these results, the ZnSe etching in the etchant could be summarized as the following equation:

$$8H_2SO_4 + 2KMnO_4 + 5ZnSe = 5Se + 5ZnSO_4 + 2MnSO_4 + K_2SO_4 + 8H_2O. \quad (1)$$

To control the dimensions of microlens fabrication by femtosecond laser assisted chemical etching, we investigated the relationship between the diameter and height of the microlens and etching time. As shown in Fig. 3(a), the laser power was 3mW, the diameter and sag height of the microlens increased with the removal of laser-modified region and reached a maximum value when complete removal of the modified region took place. Then, the microlens array was formed on the ZnSe surface. The geometrical parameters that determine the focal length (*f*) and numerical aperture (*NA*) of the microlens, can

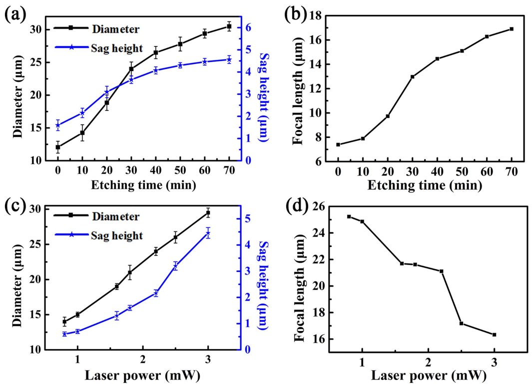

Fig. 3. Dependences of diameter and sag height (a) and the calculated focal length (b) of microlens versus the etching time. The evolution of the diameter and sag height (c) and the calculated focal length (d) of microlens versus the laser power.

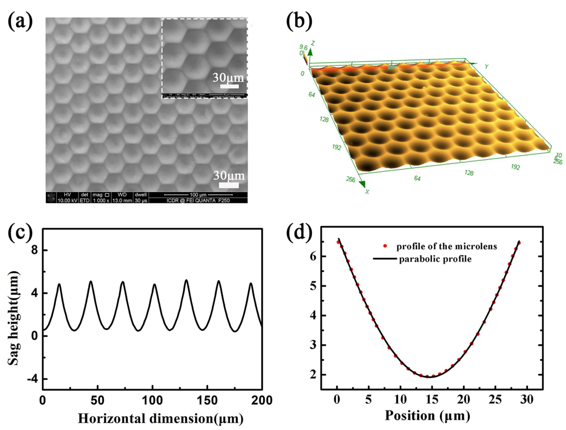

Fig. 4. Characterization of the concave microlens array on a ZnSe surface. (a) The SEM image. (b) 3D profiles and (c) the cross-section of the microlens array. (d) The measured profiles of the MLAs and the fit of the parabolic profile.

be calculated by the following formulas [20]:

$$f = -\frac{4h^2 + D^2}{8h(n-1)} \quad NA = \frac{D}{2f} \tag{2}$$

where h is the sag height, D is the diameter and $n = 2.63$ is the refractive index of the ZnSe. The calculated focal length of the microlens increased with the etching time, as shown in Fig. 3(b). To study how the laser irradiation conditions affected the dimensions of the microlenses, we fabricated microlenses at different laser powers. The results are shown in Fig. 3(c) and Fig. 3(d). The diameter and height of the microlens were positively correlated with the laser power, and higher powers yielded smaller focal length.

Fig. 4(a) and 4(b) show the SEM image of the fabricated concave MLAs and the 3D morphology data which was measured by a laser confocal scanning microscope (LCSM, Olympus LEXT OLS400). The images show that the concave microlens have a perfect surface quality and uniformity. To demonstrate the uniformity of the fabricated microlenses, different regions were measured and the data were treated with statistical processing and analysis, shown in Fig. 4(c). Consequently, the microlenses with the aperture diameter 29.5μm and sag height 4.46μm were fabricated at a laser of 3mW, etching time of 70min. The microlenses were arranged in a periodic array with a fill factor close to 100%. The obtained f and NA can be calculated as 16.33μm and 0.9, respectively.

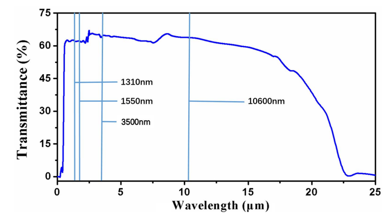

Fig. 5. Transmission properties of the IR MLA.

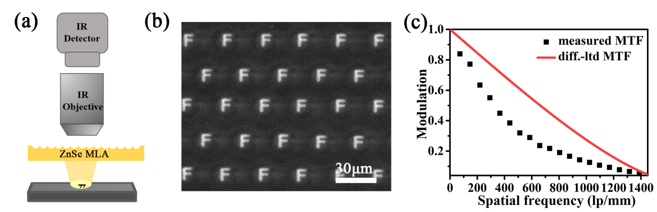

Fig. 6. (a) Scheme of the imaging setup. (b) The infrared images of the letter "F" with an infrared CCD. (c) The calculated MTF.

Moreover, to investigate the surface profile of the concave microlens, we fitted its cross-sectional profile with conic curves. Fig. 4(d) shows the cross-sectional profile of the microlens (line) and the ideal parabola (dots). The theoretical fitting results show that the root-mean-square deviation between the measured cross-sectional profile and the ideal parabola was less than 70nm. It is reasonable to identify the cross-sectional profile as a parabola.

The transmittance of the IR MLA has been measured by an UV-VIS-NIR spectrophotometer (Perkinelmer Lambda750) and Fourier transform infrared spectrometer (Thermofisher Nicolet iS10), as shown in Fig. 5. The transmission spectrum shows relatively high transmittance in visible, the near infrared and middle infrared region from 0.76μm~22μm. Especially, it shows remarkable transparency in the near infrared and middle infrared windows, such as 1310nm for InGaAs semiconductor lasers, 1550 nm for Er^+-doped fiber lasers, 3500nm for Cr:CdSe lasers and 10600nm for CO_2 lasers. This may predict the potential application of the device in the near infrared and middle infrared region.

To demonstrate the IR imaging performance of the MLA, we used an IR microscopy system comprising an illumination light (1500nm), an IR charge-coupled device (CCD) camera (Raptor, OW1.7-CL-320), a 3D translation stage and an IR objective lens (Nikon, Plan Apo NIR), as shown in Fig. 6(a). In the measurement, a transparent film printed with the capital letter "F" was positioned between the illumination light and the MLA. An arrayed image of the mask was formed by the MLA, and was magnified by an IR microscope object lens, the infrared images of the letter "F" were obtained by the infrared CCD camera, as shown in Fig. 6(b). The imaging performance of the ZnSe MLA has also been evaluated by a quantitative test of the MTF based on the measured point spread function (PSF) [21]. We used the same setup as in paper [11]. A microscope (Nikon ECLOPSE LV100ND) was equipped with an IR optimized objective. A pinhole with diameter of 100 um was placed at the object plane of the collimator lens of Köhler illumination, and the IR MLA on the XY stage was illuminated by the collimated IR beam. The imaginary focal spot through the single microlens is sampled are received by CCD [22]. Then, the MTF is achieved by Fourier transform of the recorded PSF, as shown in Fig. 6(c). The modulations of the microscope system and the imaging sensor have already

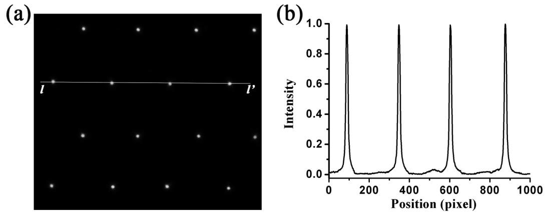

Fig. 7. (a) The false bright image of the foci array captured with a CCD sensor. (b) The normalized intensity distribution obtained along line *ll'*.

been corrected. Because the ZnSe material has relatively high refractive index, thus the fabricated ZnSe microlens shows high numerical aperture and spatial resolution. The measured MTF indicated a practical spatial resolution of 700 lp/mm by an empirical modulation contrast criterion of 0.2 [23]. The high-performance imaging quality of the MLA demonstrated the good surface smoothness and excellent uniform of the microlenses. Meanwhile, it predicts a potential in ultra-high resolution IR imaging with the proposed ZnSe MLA.

According to geometrical optics, a light beam will diverge after propagating through a concave refractive microlens, which does not have a real focal point in the light field. Even so, a focal point can still be obtained by the setup [24], [25]. The MLA was mounted on a sample holder, and the broadband light illuminated the sample from the backside. A microscope objective lens (Nikon, NA = 0.8) was used to sample the virtual focal point of the light propagating through the microlenses and CCD camera was used to capture the microscopic images, shown in Fig. 7(a). The average focal length f of the microlens was measured from ten microlenses to be $16\mu m \pm 3\mu m$, which agrees with the calculated value. To quantify the optical focusing, the cross-sectional intensity distribution of the focusing spots was calculated along the line *ll*' and shown in Fig. 7(b). Due to the uniform size of the fabricated microlenses, the light intensity distribution at the focus of the array was identical for each lenslet.

IV. Conclusion

In summary, the femtosecond laser and chemical etching have been successfully used for fabrication of the microlens arrays (MLAs) on the ZnSe for IR optics application. The related etching mechanism, like the optimized laser exposure and etchant parameters, was established. In the etching process, $KMnO_4$ in H_2SO_4 is selected as an oxidizing route to remove the modified region. The chemical reaction equation is obtained by analyzing the types and valence changes of elements during the chemical reaction. The diameter and the height of the microlens as well as the focal length can be adjusted by laser power and etching time. Based on this method, uniform close-packed MLAs with minimized volume and high transparency at wavelengths of $0.76 \sim 22\mu m$ were realized. The MLAs have relatively good topography and surface quality. The MTF, imaging test and optical-focusing test confirm its outstanding IR imaging. All the evidence shows the fabricated IR MLA to be a competitive device for IR imaging and IR sensing application.

Acknowledgment

The SEM work was done at International Center for Dielectric Research (ICDR), Xi'an Jiaotong University.

References

[1] A. Orth and K. Crozier, "Microscopy with microlens arrays: High throughput, high resolution and light-field imaging," *Opt. Express*, vol. 20, no. 12, pp. 13522–13531, Jun. 2012.

[2] A. Deutsch *et al.*, "Microplate cell-retaining methodology for high-content analysis of individual non-adherent unanchored cells in a population," *Biomed. Microdevices*, vol. 8, no. 4, pp. 361–374, Jun. 2006.

[3] M. Mukaida and J. Yan, "Ductile machining of single-crystal silicon for microlens arrays by ultraprecision diamond turning using a slow tool servo," *Int. J. Mach. Tools Manuf.*, vol. 115, pp. 2–14, Apr. 2017.

[4] J. Albero, L. Nieradko, C. Gorecki, H. Ottevaere, V. Gomez, H. Thienpont, J. Pietarinen, B, Päivänranta, and N.Passilly, "Fabrication of spherical microlenses by a combination of isotropic wet etching of silicon and molding techniques," *Opt. Express*, vol. 17, no. 8, pp. 6283–6292, Apr. 2009.

[5] Z. Deng *et al.*, "Fabrication of large-area concave microlens array on silicon by femtosecond laser micromachining," *Opt. Lett.*, vol. 40, no. 9, pp. 1928–1931, May 2015.

[6] Z.-H. Chen, L. Liang, Y. Wang, and Y. Yang, "Spatial remote luminescence enhancement by a half-cylindrical au groove," *J. Mater. Chem. C*, vol. 4, no. 47, pp. 11321–11327, 2016.

[7] Z.-H. Chen, H. Shi, Y. Wang, Y. Yang, S. Liu, and H. Ye, "Sharp convex gold grooves for fluorescence enhancement in micro/nano fluidic biosensing," *J. Mater. Chem. B*, vol. 5, no. 44, pp. 8839–8844, 2017.

[8] Z.-H. Chen, H. Quan, Y. Wang, and Y. Yang, "Enhanced far-field directional luminescence emission by a hybrid structure consisting of silver channel and microlens," *IEEE Photon. J.*, vol. 11, no. 3, Jun. 2019, Art. no. 2200708.

[9] J. Q. Yu *et al.*, "Droplet optofluidic imaging for bacteriophage detection via co-culture with host cell escherichia coli," *Lab Chip*, vol. 14, no. 18, pp. 3519–3524, Jun. 2014.

[10] G. Molar-Velázquez, F. J. Renero-Carrillo, and W. Calleja-Arriaga, "Two-dimensional optical micro-scanner on silicon technology," *Optik*, vol. 121, no. 9, pp. 843–846, May 2010.

[11] F. Liu, Q. Yang, F. Chen, F. Zhang, H. Bian, and X. Hou, "Low-cost high integration IR polymer microlens array," *Opt. Lett.*, vol. 44, no. 7, pp. 1600–1602, Apr. 2019.

[12] X. B. Zhang, K. L. Ha, and S. K. Hark, "Selenium-related luminescent centers in metalorganic chemical-vapor-phase deposition grown ZnSe epilayers on GaAs," *Appl. Phys. Lett.*, vol. 79, no. 8, pp. 1127–1129, Aug. 2001.

[13] S. K. Yadav and R. Ramprasad, "Strain-assisted bandgap modulation in zn based II-VI semiconductors," *Appl. Phys. Lett.*, vol. 100, no. 24, Jun. 2012, Art. no. 241903.

[14] X.-Q. Liu *et al.*, "Dry-etching-assisted femtosecond laser machining," *Laser Photon. Rev.*, vol. 11, no. 3, May 2017, Art. no. 1600115.

[15] D. Wu *et al.*, "High numerical aperture microlens arrays of close packing," *Appl. Phys. Lett.*, vol. 97, no. 3, Jul. 2010, Art. no. 031109.

[16] X. Liu *et al.*, "Optical nanofabrication of concave microlens arrays," *Laser Photon. Rev.*, vol. 13, no. 5, May 2019, Art. no. 1800272.

[17] C. Luo, H. Wang, L. Liao, C. Yang, and T. Kobayashi, "Preparation of ZnSe nanoparticles with femtosecond laser," in *Proc. Int. Quantum Electron. Conf. Conf. Lasers Electro-optics Pacific Rim*, 2011, pp. C764.

[18] S. López-Marino *et al.*, "ZnSe etching of zn-rich Cu2ZnSnSe4: An oxidation route for improved solar-cell efficiency," *Chem. Eur. J.*, vol. 19, no. 44, pp. 14814–14822, Oct. 2013.

[19] E. M. Gavrishchuk, E. Y. Vilkova, O. V. Timofeev, U. P. Borovskikh, and E. L. Tikhonova, "Etching behavior of CVD zinc selenide in inorganic acid solutions," *Inorganic Mater.*, vol. 43, no. 6, pp. 579–583, Jun. 2007.

[20] X. Liu *et al.*, "Ultra-smooth micro-optical components of various geometries," *Opt. Lett.*, vol. 44, no. 10, pp. 2454–2457, May 2019.

[21] A. Bräckner, J. Duparré, R. Leitel, P. Dannberg, A. Bräuer, and A. Tännermann, "Thin wafer-level camera lenses inspired by insect compound eyes," *Opt. Express*, vol. 18, no. 24, pp. 24379–24394, Nov. 2010.

[22] X. Liu, S. Yang, L. Yu, Q. Chen, Y. Zhang, and H. Sun, "Rapid engraving of artificial compound eyes from curved sapphire substrate," *Adv. Funct. Mater.*, vol. 29, no. 18, May 2019, Art. no. 1900037.

[23] F. Liu *et al.*, "IR artificial compound eye," *Adv. Opt. Mater.*, vol. 8, no. 4, Feb. 2020, Art. no. 1901767.

[24] H. Bian *et al.*, "Direct fabrication of compound-eye microlens array on curved surfaces by a facile femtosecond laser enhanced wet etching process," *Appl. Phys. Lett.*, vol. 109, no. 22, Nov. 2016, Art. no. 221109.

[25] Z. Deng *et al.*, "Dragonfly-Eye-Inspired artificial compound eyes with sophisticated imaging," *Adv. Funct. Mater.*, vol. 26, no. 12, pp. 1995–2001, Mar. 2016.